



# Incorporation of Fe-phthalocyanines into a porous organic framework for highly efficient photocatalytic oxidation of arylalkanes



Wei-Long He, Chuan-De Wu\*

State Key Laboratory of Silicon Materials, Center for Chemistry of High-Performance & Novel Materials, Department of Chemistry, Zhejiang University, Hangzhou, 310027, PR China

## ARTICLE INFO

### Keywords:

Biomimetic  
Metallophthalocyanines  
Photocatalysis  
Porous organic polymers  
Self-aggregation

## ABSTRACT

Metallophthalocyanines (MPcs) are a class of bioinspired artificial aromatic macrocycles with unique properties of excellent visible light absorption and remarkable photocatalytic activity. However, the catalytic efficiency of MPcs is heavily diminished by strong intermolecular  $\pi$ - $\pi$  self-aggregation. To solve the self-aggregation problem and realize highly efficient photocatalysis, we develop a strategy to immobilize MPc moieties into porous organic polymers (POPs). The solvothermal reaction between four-branched tetra-amine FePc (T AFP) and three-connected 1,3,5-triformylbenzene (TFB) results in a 3D porous organic material CZJ-30, consisting of highly photoactive FePc moieties. CZJ-30 demonstrates high photoactivity and stability in photoxidation of arylalkanes under visible light irradiation, in which 95% ethylbenzene conversion, > 99% acetophenone selectivity and 11,950 turnovers have been realized for photoxidation of ethylbenzene. Compared with its molecular counterpart Fe-Pc, CZJ-30 exhibits superior photocatalytic properties, and offers significant superiority of robustness to self-oxidation and simple recovery for recycling with persisted high photocatalytic efficiency.

## 1. Introduction

Metallophthalocyanines (MPcs), consisting of 18-electron co-planar aromatic macrocycles, are a class of bioinspired artificial molecules that are associated with the biological functions of metalloporphyrins, such as hemoglobin for oxygen transport, peroxidase for oxidation, cytochrome for electron transport, chlorophyll for photosynthesis and catalase for hydrogen peroxide decomposition [1,2]. Attributed to their unique physicochemical, electronic and optical properties, MPcs have been realized applications in numerous fields [3]. Being the analogues of heme cofactors in cytochromes P450, MPcs exhibited the capability of prompting the spin-state transition of molecular oxygen from ground-state ( $^3\text{O}_2$ ) to highly active singlet ( $^1\text{O}_2$ ) [4]. Inspired by their unique properties, MPcs have been targeted as a class of efficient catalysts for aerobic oxidation of a variety of organic molecules [5–13]. However, compared with those of metalloporphyrins, the catalytic applications of MPcs are significantly diminished because the large  $\pi$ -conjugation macrocycles are prone to form densely packed cofacial aggregates through strong intermolecular  $\pi$ - $\pi$  interactions, which would heavily block the accessibility of central active metal sites to reactant molecules [13]. To prohibit the self-association of MPcs, heterogenization has been extensively investigated by covalent grafting, encapsulating and impregnating these macrocycles into porous materials,

such as microporous zeolites, mesoporous silicas, carbon materials and organic polymers [14–19]. Even though the self-aggregation probability of MPcs was greatly minimized by dispersing into porous solid materials, however, inhomogeneous distribution and pendency inevitably resulted in low density of MPc active sites and low space utilization with partially aggregated MPc moieties.

Porous organic polymers (POPs) are an emerging class of porous materials connected by covalent organic bonds, which present high chemical and thermal stability, and tunable properties for applications in many fields [20–29]. By tuning the connecting points on the rigid macrocycles, MPcs have been incorporated into two-dimensional (2D) POPs by covalent bond cross linkage [30–33]. However, because the macrocycles in 2D POPs are stacked by strong  $\pi$ - $\pi$  stacking interactions, the active Pcs metal sites are inaccessible to reactant molecules. To endow the Pcs metal sites accessible to reactant molecules for highly efficient catalysis, cross-connection of MPcs into three-dimensional (3D) frameworks of POPs is highly desired [34,35]. Because the structures of POPs are largely depending on the reticular chemistry principle, the connectivities, geometries and branches of organic building synthons have been demonstrated as the essential elements for the rational design and construction of 3D POPs [26–28]. To synthesize stable and porous 3D organic materials consisting of substrate accessible MPc sites for highly efficient heterogeneous photocatalysis, we reacted four-

\* Corresponding author.

E-mail address: [cdwu@zju.edu.cn](mailto:cdwu@zju.edu.cn) (C.-D. Wu).

branched tetra-amine FePc (T AFP) with trigonal 1,3,5-triformylbenzene (TFB) in a simple one-pot procedure under solvothermal conditions. The dehydration between T AFP and TFB produced an extended 3D porous POP material CZJ-30, consisting of self-loaded FePc moieties that are cross-linked by imine bonds. The inter-connections between the four-branched and three-connected rigid moieties forced the FePc moieties to point to different directions, which prevented the  $\pi$ - $\pi$  co-facial stacking in the resulted polymeric material. Exposure of FePc active sites inside the pores of CZJ-30 enables them easily accessed to reactant molecules transferred from the pore channels. Photocatalytic experiments demonstrated that CZJ-30 was capable of activating molecular oxygen irradiated by visible light, which exhibited high efficiency, excellent selectivity, broad substrate applicability and good reusability in photo-oxygenation of the inert  $sp^3$  C–H bonds of arylalkanes.

## 2. Experimental

### 2.1. Materials and methods

All of the chemicals were obtained from commercial sources and used without further purification, except 1,3,5-triformylbenzene (TFB) and tetra-amine FePc (T AFP) were prepared according to the literature [36,37]. FT-IR spectra were collected from KBr pellets on an FTS-40 spectrophotometer. Thermogravimetric analysis (TGA) was carried out under  $N_2$  atmosphere on a NETZSCH STA 409 PC/PG instrument at a heating rate of  $10\text{ }^{\circ}\text{C min}^{-1}$ . UV-vis spectra were recorded on a TU-1901 spectrophotometer. GC–MS data were recorded on a SHIMADZU GCMS-QP2010. Powder X-ray diffraction (PXRD) data were recorded on a RIGAKU D/MAX 2550/PC for Cu K $\alpha$  radiation ( $\lambda = 1.5406\text{ \AA}$ ). A Micromeritics ASAP 2020 surface area analyzer was used to measure  $CO_2$  gas adsorption/desorption isotherms. X-ray photoelectron spectra (XPS) were recorded on a VG ESCALAB MARK II machine. Inductively coupled plasma mass spectrometry (ICP-MS) was performed on an X-Series II instrument. Scanning electron microscopy (SEM) image was recorded on a Hitachi S-4800 equipment. Transmission electron microscopy (TEM) equipped with an energy dispersive X-ray (EDX) detector was recorded on a JEM 2100F equipment, and the sample was deposited onto an ultrathin carbon film on copper grids. The photoelectrochemical current responses were measured on a CHI 660E electrochemical workstation.

### 2.2. Synthesis of CZJ-30

A mixture of T AFP (18.8 mg, 0.03 mmol), TFB (6.5 mg, 0.04 mmol) and aqueous acetic acid (3 mL, 12 M) in a mixed solvent of dioxane (10 mL), pyridine (2.5 mL) and mesitylene (2 mL) was heated at  $160\text{ }^{\circ}\text{C}$  for 72 h. Dark green solid powder was collected by filtration, and washed with alcohol and acetone several times. The solid powder was activated by immersing in anhydrous acetone for 24 h, and dried at  $65\text{ }^{\circ}\text{C}$  under vacuum for 12 h. FT-IR (KBr pellet,  $\nu/\text{cm}^{-1}$ ): 1606(s), 1467(w), 1401(w), 1335(w), 1232(s), 1127(w), 1084(w), 829(w), 750(s), 669(w).

### 2.3. A typical procedure for the photocatalytic oxidation of arylalkanes

Ethylbenzene (0.3 mmol), CZJ-30 (0.001 mmol based on FePc) and *N*-hydroxyphthalimide (NHPI) (0.03 mmol) in acetonitrile (2 mL) were stirred at room temperature under the irradiation of a 350 W Xe lamp for 24 h in the presence of  $O_2$  (1 atm). The solid was recovered by centrifugation, and thoroughly washed with MeOH, THF,  $CH_3CN$  and  $Et_2O$  several times. The recovered solid was reused in the successive run. The identity of the product was determined by GC–MS (Figs. S11–S26), and compared with the authentic sample analyzed under the same conditions, while the yield was obtained by GC analysis using a flame-ionization detector (FID) with a capillary SE-54 column in the

presence of an internal standard of naphthalene.

### 2.4. Study of the turnover numbers (TONs) for the photooxidation of ethylbenzene catalyzed by CZJ-30

Ethylbenzene (50 mmol), CZJ-30 (0.001 mmol based on FePc) and NHPI (5 mmol) in acetonitrile (80 mL) were stirred at room temperature under the irradiation of a 350 W Xe lamp in the presence of  $O_2$  (1 atm). The aliquots were regularly taken out for GC analysis to determine the conversion of ethylbenzene, the yield of acetophenone, and TONs (TON is defined as the mole ratio of the substrate converted to the FePc unit).

### 2.5. A typical procedure for the substrate absorption experiments

A sample of acetone-exchanged CZJ-30 (5 mg) was treated under vacuum at  $65\text{ }^{\circ}\text{C}$  for 12 h. The evaluated sample was subsequently immersed in ethylbenzene (1.0 mL) at room temperature for 12 h, and centrifugated. The recovered solid was thoroughly washed with ethyl ether to remove the surface adsorbed molecules, which was subsequently submersed in  $CH_3CN$  under stirring for 18 h. The supernatant liquid was subjected to GC analysis.

### 2.6. A typical procedure to study the chemical species adsorbed inside the pores of CZJ-30 during photooxidation of ethylbenzene

Ethylbenzene (0.3 mmol), CZJ-30 (0.001 mmol based on FePc) and NHPI (0.03 mmol) in acetonitrile (2 mL) were stirred at room temperature under the irradiation of a 350 W Xe lamp for 9 h in the presence of  $O_2$  (1 atm). The solid was recovered by centrifugation, and thoroughly washed with  $Et_2O$ . The solid was immersed in acetonitrile for 18 h, and centrifugated. The supernatant liquid was subjected to GC–MS analysis and compared with the authentic samples analyzed under the same conditions.

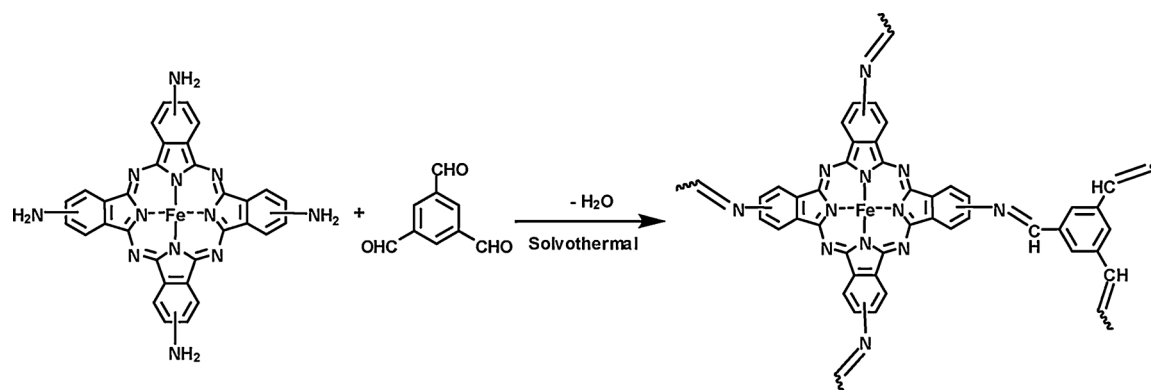
### 2.7. Photoelectrochemical measurement

The photoelectrochemical properties of CZJ-30 were studied on a CHI 660E electrochemical workstation using a standard three-electrode system. The working electrode was prepared according to the following procedure: 3 mg of CZJ-30 was ground in a mixture of  $EtOH$  (1 mL) and aqueous nafion (5%; 0.1 mL) for 10 min to produce slurry. The as-obtained slurry was spread onto the conductive surface of the fluorine-doped tin oxide (FTO) glass ( $10 \times 10\text{ mm}^2$ ) to form a film, and dried in air to obtain the CZJ-30/FTO working electrode. Tetrabutylammonium perchlorate acetonitrile solution (0.1 M) was used as the electrolyte, and platinum wire and saturated calomel electrode (SCE) served as the counter electrode and the reference electrode, respectively. The photocurrent responses were measured in 0.1 M tetrabutylammonium perchlorate acetonitrile solution (25 mL) consisting of ethylbenzene (0.3 mmol) and NHPI (0.03 mmol) in the presence of  $O_2$  (1 atm) at room temperature under the irradiation of a 350 W Xenon lamp with a 400 nm cut-off filter. Amperometric  $I$ - $t$  curves were obtained at 0 V (vs. SCE electrode) with light on-off switches of 30 s.

## 3. Results and discussion

CZJ-30 was synthesized by reversible condensation reaction between TFB and T AFP in a mixed solvent of mesitylene, 1,4-dioxane, pyridine and aqueous acetic acid (Scheme 1). According to the reticular chemistry principle, the formation of C=N imine bonds between the three-connected and four-branched organic building synthons should result in CZJ-30 as an extended 3D porous framework material, consisting of uniformly dispersed catalytic-active FePc moieties.

As shown in Fig. S1, the synthetic procedure for CZJ-30 was monitored by UV-vis absorption spectroscopy. When acetic acid was added



Scheme 1. Schematic representation of the synthetic procedure for CZJ-30.

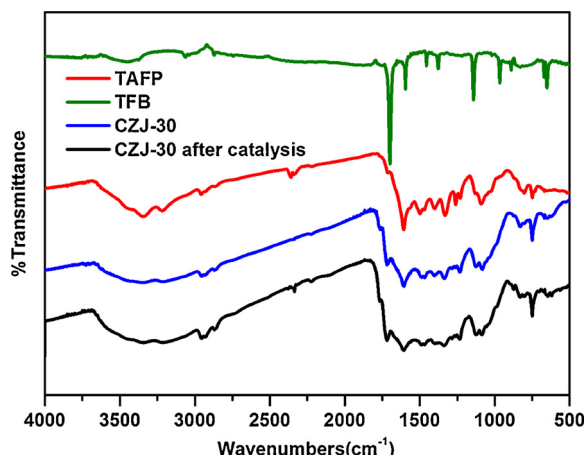


Fig. 1. FT-IR spectra of 1,3,5-triformylbenzene (TFB), tetra-amine FePc (TAFP), CZJ-30 and recovered CZJ-30 after catalysis.

to the TAFP solution of pyridine, mesitylene and 1,4-dioxane, the absorption peak of the solution was blue-shifted from 705 to 673 nm, because protonation of the amino groups in TAFP would withdraw electrons from the phthalocyanine macrocycles. When TFB was added to the mixture, the absorption peak decreased gradually, and the color of the reaction solution gradually changed from green to colorless. CZJ-30 was obtained as dark green powder which is insoluble in water and common organic solvents, such as alcohols, acetone, chloroform, acetonitrile, DMF and DMSO. The as-synthesized CZJ-30 was activated by immersing in dry acetone to exchange the included solvent molecules, and further dried at 65 °C under vacuum for 12 h. FT-IR spectrum of CZJ-30 clearly showed that the C=N stretching vibration band of imine moieties is centered at 1232 cm<sup>-1</sup> (Fig. 1) [38]. The bands at 1606, 1467, 1401, 1335, 1127 and 1084 cm<sup>-1</sup> are attributed to the phthalocyanine ring skeleton. The characteristic signal for carbonyl ν<sub>C=O</sub> stretching vibration (1700 cm<sup>-1</sup>) was almost disappeared in the FT-IR spectrum of CZJ-30, suggesting that most of the aldehyde moieties have been reacted with the amino units in TAFP during formation of the polymeric material [39]. Similarly, the characteristic bands of the ν<sub>as</sub> and ν<sub>s</sub> stretching vibrations of amino groups at 3346 and 3218 cm<sup>-1</sup> almost disappeared, indicating that most of the amino groups in TAFP have been consumed during the condensation reaction. The UV-vis diffuse reflectance spectroscopy analysis showed that there are the characteristic Pc absorption bands in the spectrum of CZJ-30 (Fig. S2). The absorption band at 717 nm is ascribed to the characteristic Q-band of FePc moieties, which is attributed to the π-π\* transition from the highest occupied molecular orbital (HOMO) to the lowest unoccupied molecular orbital (LUMO) of the FePc moieties [40]. The optical band gap of CZJ-30 was evaluated from the tangent of the curve plotted using

the Tauc plot equation, which resulted in the band gap energy (Eg) of 2.2 eV [41]. X-ray photoelectron spectroscopy (XPS) of CZJ-30 showed that the binding energy for Fe 2p<sub>3/2</sub> is centered at 710.4 eV, which is close to the value observed in the literature (Fig. S4) [42,43].

The morphology of CZJ-30 was studied by scanning electron microscopy (SEM) and transmission electron microscopy (TEM) (Figs. S5 and S6). The SEM image showed that the particle sizes of CZJ-30 are not uniform with irregular shapes, which are in the range of 1–5 μm. It can be seen that the particles with rough surfaces are composed of loosely agglomerated nanoparticles, which are favorable for the diffusion of reactant and product molecules during photocatalysis. The TEM image of CZJ-30 exhibited clear agglomerated particle profile with irregular shapes which are in agreement with the SEM result. The EDX spectrum of CZJ-30 indicated the existence of C, N, O and Fe elements. The elemental mapping images clearly showed the homogeneous distribution of C, N, O and Fe elements in CZJ-30. Powder X-ray diffraction (PXRD) profile demonstrated the amorphous character of CZJ-30, which should be ascribed to the amino groups that are randomly located on the FePc macrocycles (Fig. S7). Thermogravimetric analysis (TGA) revealed that CZJ-30 could be stable up to 420 °C (Fig. S8). The permanent porosity of CZJ-30 has been examined by CO<sub>2</sub> gas adsorption measurements at 273 K (Fig. S9). After the as-synthesized sample of CZJ-30 was acetone-exchanged and heated at 90 °C under vacuum for 12 h, the activated solid sample took up 35.7 cm<sup>3</sup> g<sup>-1</sup> CO<sub>2</sub> at 273 K and 1 bar. Nonlocal density functional theory analysis of the CO<sub>2</sub> adsorption isotherm resulted in a microporous surface area of 780 m<sup>2</sup> g<sup>-1</sup>. The access of different solvent molecules to the inside pores of activated CZJ-30 was confirmed by solvent sorption studies. When the activated samples of CZJ-30 were immersed in a series of different solvents at room temperature for 12 h, GC analysis of the supernatants indicates that the activated CZJ-30 can readily take up large amounts of different solvent molecules such as toluene, ethylbenzene, phenylpropane, acetophenone, propiophenone, acetone and ethanol (Fig. 2).

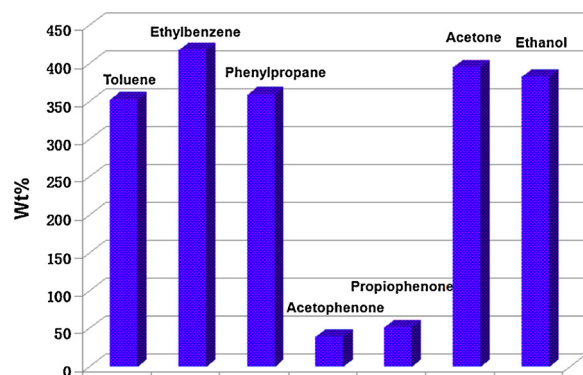


Fig. 2. Illustration of the sorption ability of CZJ-30 as probed by GC.

Apparently, the *Pc*-Fe active sites in CZJ-30 are readily accessible to different small reactant molecules transferred through the pore channels during catalysis.

Selective oxidation of hydrocarbons by molecular oxygen is a significant process in the chemical industry which would convert the relatively cheap hydrocarbons into valuable oxo-functionalized fine chemical products [44,45]. Even though great effort has been devoted to develop efficient approaches for direct oxygenation of alkanes with molecular oxygen, however, it remains one of the biggest challenges for the oxidation of saturated alkanes due to the inertness of  $sp^3$  C–H bonds [46,47]. The harsh reaction conditions, corrosive additives, low product selectivities and environmentally hazardous wastes do not meet the demand of sustainable green chemistry. Alternatively, photocatalysis may contribute an efficient pathway to solve these problems with the unique advantages of operating at room temperature and atmosphere pressure irradiated by renewable solar light [48,49]. Since MPCs are a class of efficient photosensitizers with excellent visible light absorption, remarkable photoactivity and unique ability to photo-generate reactive singlet oxygen from ground-state molecular oxygen, CZJ-30 should be highly active for photoactivation of  $O_2$  oxidant under visible light irradiation [8]. We were therefore motivated to study the photocatalytic properties of CZJ-30 in aerobic oxidation of the inert  $sp^3$  C–H bonds in arylalkanes. The photocatalysis was performed in acetonitrile under  $O_2$  atmosphere (1 atm) in the presence of co-catalyst *N*-hydroxyphthalimide (NHPI) irradiated by visible light. As shown in Table 1 (entry 1), it is interesting that CZJ-30 efficiently prompted the photocatalytic oxidation of ethylbenzene with 95% acetophenone yield and high selectivity (> 99%). If the reaction was carried out in the dark environment, we only found a trace of the product (entry 2), which proved that the oxidation reaction is a photo-induced process. The catalytic efficiency of CZJ-30 is significantly higher than that of molecular catalyst Fe-2,3-naphthalocyaninato (Fe-Pc) under the identical conditions (entry 3). It is very interesting that the photocatalytic efficiency of the heterogeneous catalyst is significantly superior to that of the molecular catalyst. The improved photocatalytic oxidation efficiency of CZJ-30 should be ascribed to incorporation of the molecular FePc moieties into the pore matrices that would preclude them from cofacially  $\pi$ – $\pi$  stacking, and thus endow the active *Pc*-Fe sites more easily accessed than those of molecular catalysts [37].

The porous organic catalyst CZJ-30 is very stable, which can be simply recovered by centrifugation, and subsequently reused in the successive run for eight cycles with almost retained high catalytic efficiency and selectivity (Table 1, entry 4; Fig. S10). ICP-MS and UV-vis spectroscopy of the plasma after catalysis demonstrated that the FePc moieties did not leach off during the photocatalysis. Compared with those of the as-synthesized CZJ-30, IR and UV-vis spectra, and SEM, TEM, EDX and elemental mapping images indicated that the basic structure and morphology of CZJ-30 were still retained after photocatalysis, except the particle profile became smaller (Figs. 1, S2, S5 and S6). In contrast, the molecular catalyst Fe-Pc is almost deactivated at the third run (Table 1, entry 5). The above results demonstrated that immobilization of MPCs into the frameworks of POPs not only can solve the self-aggregation issue but also would avoid oxidative degradation of the MPC moieties, which significantly improved the catalytic efficiency and the sustainability, respectively. CZJ-30 also presented widespread substrate tolerance, which can photocatalytically oxidize various alkylalkanes to afford valuable arylketones under the above mentioned reaction conditions (Table 1, entries 6–12). The conversions of alkylalkanes ranged from moderate to high, depending on the steric hindrance when accessed to the active *Pc*-Fe sites on the rigid macrocycles in the pore surfaces during photocatalysis.

To check whether the catalysis chiefly occurred inside the pore space of CZJ-30, we studied the included species during photocatalytic oxidation of ethylbenzene. After the catalytic reaction proceeded for 9 h, the reaction was intentionally interrupted. The solid catalyst was collected by centrifugation, and washed with ethyl ether several times.

**Table 1**  
Photocatalytic oxidation of benzylic  $sp^3$  C–H bonds of arylalkanes.<sup>a</sup>

Entry	Substrate	Catalyst	Product	Conv. (%) <sup>b</sup>	Select. (%) <sup>b</sup>
				$O_2$ , 1 atm	Cat., $h\nu$
1		CZJ-30		95	> 99
2		CZJ-30		trace	– <sup>c</sup>
3		Fe-Pc		23	90
4		CZJ-30		92	98 <sup>d</sup>
5		Fe-Pc		6	– <sup>e</sup>
6		CZJ-30		97	86
7		CZJ-30		72	> 99
8		CZJ-30		96	> 99
9		CZJ-30		57	> 99
10		CZJ-30		86	> 99
11		CZJ-30		55	> 99
12		CZJ-30		69	> 99

<sup>a</sup> Reaction conditions: a mixture of substrate (0.3 mmol), CZJ-30 (0.001 mmol based on FePc) and NHPI (0.03 mmol) in acetonitrile (2 mL) was stirred under an  $O_2$  atmosphere (1 atm) irradiated by a 350 W Xe lamp for 24 h.

<sup>b</sup> Determined by GC-MS.

<sup>c</sup> In the dark.

<sup>d</sup> The eighth cycle.

<sup>e</sup> The third cycle.

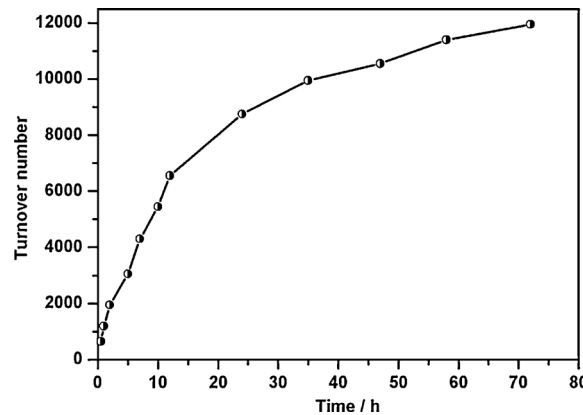


**Fig. 3.** Kinetic process for the photocatalytic oxidation of ethylbenzene by CZJ-30 irradiated under visible light.

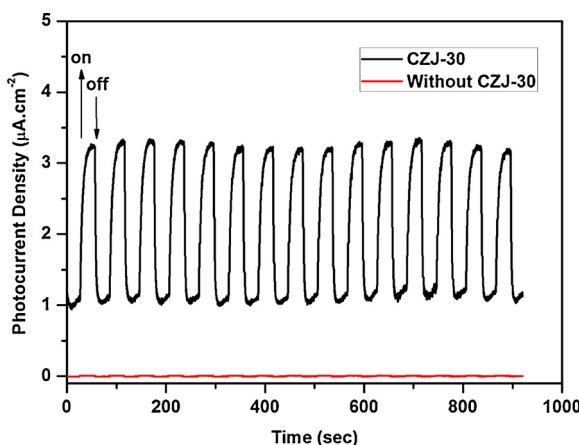


**Fig. 4.** The  $I-t$  curves of the CZJ-30/FTO electrode. The measurements were conducted at 0 V (vs. SCE electrode) under a 350 W Xenon lamp irradiation with a 400 nm cut-off filter.

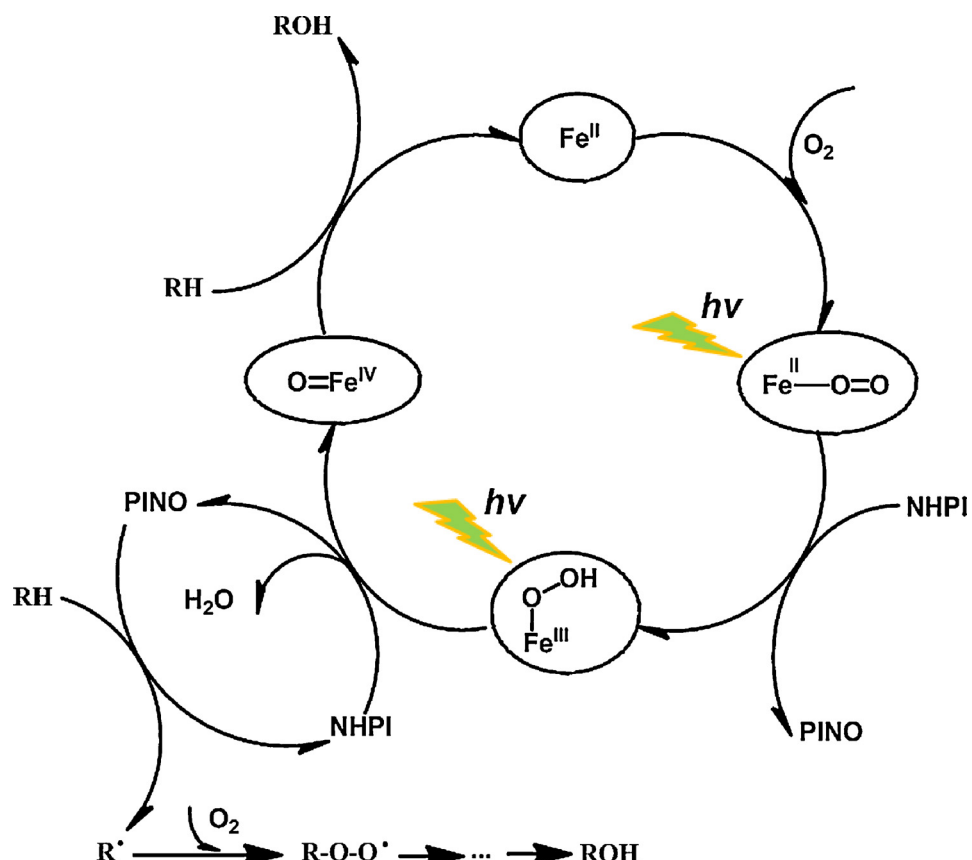
The collected solid sample was subsequently submersed in acetonitrile for 18 h to release the included species at room temperature. GC-MS analysis of the supernate indicates that almost of the released species from this reacted CZJ-30 are ethylbenzene molecules (5.2 wt%) and the released acetophenone is negligible, even though the conversion of ethylbenzene has been reached to 69%. These experimental results demonstrated that the photocatalytic oxidation of ethylbenzene mainly occurred inside the pore space of CZJ-30, and CZJ-30 exhibited selective accumulation property toward ethylbenzene reactant over acetophenone product molecules. To prove further the selective accumulation property of CZJ-30, the activated CZJ-30 was immersed in a mixture of ethylbenzene and acetophenone (v/v = 1/1) for 12 h at

room temperature. GS analysis showed that CZJ-30 preferably takes up ethylbenzene over acetophenone (6.2 mol ratio). Such preferred sorption of reactant over product molecules would facilitate the accumulation of the substrate and the release of the product molecules during photocatalysis, which should be one of the fundamental factors to explain the remarkable photocatalytic properties of CZJ-30 on oxygenation of ethylbenzene. The substrate-selective accumulation property has maximized the catalytic activity of the immobilized catalytic FePc sites in the pore matrices of CZJ-30.

Attracted by the high catalytic efficiency and stability of CZJ-30, we were motivated to enlarge the substrate scale and study the potential for practical catalytic applications. When ethylbenzene substrate was scaled up to 50 mmol, CZJ-30 still efficiently promoted this reaction under the identical photocatalytic conditions. As shown in Fig. 3, it is remarkable that the turnover number (TON) was reached to 11,950 after 72 h. The excellent photocatalytic performance was not accomplished by other photocatalysts reported so far [48,49].

The above interesting photocatalytic results prompted us to study the photoelectrochemical properties of CZJ-30. The as-synthesized solid of CZJ-30 was deposited on the fluorine-doped tin oxide (FTO) surface. The photocatalytic oxidation of ethylbenzene on CZJ-30/FTO electrode was investigated in 0.1 M  $\text{Bu}_4\text{NClO}_4$  acetonitrile solution under visible light irradiation by monitoring the photocurrent responses. As shown in Fig. 4, the maximum photo-generated current plots of the photoelectrode subjected to 30 s of on/off cycles. The photoelectrode showed evident photo-generated current responses to changes in light on/off states. The maximum photo-generated current response value of CZJ-30/FTO electrode is about  $3.3 \mu\text{A cm}^{-2}$ . In contrast, the photocurrent density of blank FTO electrode was ignorable. These results clearly demonstrated the excellent photocatalytic properties of CZJ-30 for aerobic oxidation of ethylbenzene.

According to the results obtained in this work and the catalytic



**Scheme 2.** Plausible photocatalytic mechanism for the aerobic oxidation of ethylbenzene by CZJ-30 in the presence co-catalyst NHPI.

mechanisms of enzymes, a plausible photocatalytic mechanism by CZJ-30 was proposed as shown in **Scheme 2** [50]. It has been known that  $\text{Pc-Fe}^{\text{II}}$  would easily bond with a labile dioxygen to form  $\text{Pc-Fe}^{\text{II}}-\text{O}=\text{O}$  complexation species [13]. Excited under visible light irradiation, the photosensitive FePc moieties would absorb photons to create charge-separated excited states, consisting of electron ( $e^-$ ) and hole ( $h^+$ ) pairs. The photo-generated hole is easily captured by the reductive NHPI to prompt electron-hole separation, whereas NHPI was oxidized to phthalimide-*N*-oxy (PINO) radical and  $\text{H}^+$ . Meanwhile, the photo-generated electron would be prompted to migrate to the  $\text{Pc-Fe}^{\text{II}}-\text{O}=\text{O}$  site for the formation of hydroperoxo intermediate  $\text{Pc-Fe}^{\text{III}}-\text{O}-\text{OH}$ , and then oxo-metal intermediate  $\text{Pc-Fe}^{\text{VI}}=\text{O}$ , which realized molecular oxygen activation. The oxo-metal  $\text{Pc-Fe}^{\text{VI}}=\text{O}$  species is highly reactive, which would insert the oxygen atom into the methylene  $\text{sp}^3\text{C-H}$  bond of ethylbenzene to realize aerobic oxidation. Compared with the catalytic oxidation reactions which required sacrificial agents, e.g. aldehydes, the present photocatalytic system is remarkable, because NHPI was not simply performed as the sacrificial electron donor. PINO, the hydrogen-abstracted product of NHPI, is also highly reactive, which would abstract hydrogen from ethylbenzene to return to NHPI, and initiate the radical-intermediated aerobic oxidation process [51,52]. In short, the photocatalytic aerobic oxidation is a complicated process by synergistic work between multiple species, which exhibited high catalytic efficiency in photoxidation of arylalkanes.

#### 4. Conclusions

In summary, for the intention to solve the self-aggregation issue of MPCs and realize highly efficient photocatalysis, we developed a strategy to synthesize 3D porous organic material CZJ-30 by interconnection of four-branched FePc moieties and three-connected TFB bridges. According to the reticular chemistry principle, the rigid connections between these multiple-branched building synthons avoided the FePc macrocycles from cofacially oriented  $\pi-\pi$  stacking, which endowed the  $\text{Pc-Fe}$  active sites easily accessed to reactant molecules inside the pore space that were transferred through the open channels. CZJ-30 demonstrated significantly higher photocatalytic activity and stability than its molecular counterpart in aerobic oxidation of arylalkanes irradiated by visible light. This work showed that rational design and modification of the connecting points on MPCs would control the orientation of MPC moieties in the frameworks of resulted POPs and thus significantly improve the catalytic activity by improving the access of active sites to reactant molecules. Additionally, the catalytic efficiency can be significantly improved by the unique selective accumulation property of the inside pores in CZJ-30 toward substrate over product molecules.

#### Acknowledgement

This work was financially supported by the National Natural Science Foundation of China (grant nos. 21525312 and 21373180).

#### Appendix A. Supplementary data

Supplementary material related to this article can be found, in the online version, at doi:<https://doi.org/10.1016/j.apcatb.2018.04.055>.

#### References

- [1] B. Grimm, R.J. Porra, W. Ruediger, H. Scheer, *Chlorophylls and Bacterio Chlorophylls: Biochemistry, Biophysics, Functions and Applications*, Springer, Dordrecht, 2006.
- [2] P.C. Lo, X. Leng, D.K.P. Ng, *Coord. Chem. Rev.* 251 (2007) 2334.
- [3] G. Bottari, G. de la Torre, D.M. Guldi, T. Torres, *Chem. Rev.* 110 (2010) 6768.
- [4] C. Maria, D. Rosa, C. Robert, *Coord. Chem. Rev.* 233 (2002) 351.
- [5] P. Ramacharyulu, R. Muhammad, J. Praveen Kumar, G. Prasad, P. Mohanty, *Phys. Chem. Chem. Phys.* 17 (2015) 26456.
- [6] E. Vargas, R. Vargas, O. Nunez, *Appl. Catal. B* 156 (2014) 8.
- [7] M. Gao, N. Li, W. Lu, W. Chen, *Appl. Catal. B* 147 (2014) 805.
- [8] M. Mahyari, M.S. Laeini, A. Shaabani, *Chem. Commun.* 50 (2014) 7855.
- [9] A. Aktas, I. Acar, E.T. Saka, Z. Biyiklioglu, *J. Organomet. Chem.* 1–7 (2016) 815.
- [10] X. Zhang, L. Yu, C. Zhuang, T. Peng, R. Li, X. Li, *ACS Catal.* 4 (2014) 162.
- [11] S.M. Paradine, M.C. White, *J. Am. Chem. Soc.* 134 (2012) 2036.
- [12] I.Y. Skoblev, E.V. Kudrik, O.V. Zalomaeva, F. Albrieux, P. Afanasyev, O.A. Kholdeev, A.B. Sorokin, *Chem. Commun.* 49 (2013) 5577.
- [13] A.B. Sorokin, *Chem. Rev.* 113 (2013) 8152.
- [14] G. Bottari, G. de la Torre, T. Torres, *Acc. Chem. Res.* 48 (2015) 900.
- [15] J.R. Hu, H.Y. Liu, L.L. Wang, N. Li, T.F. Xu, W.Y. Lu, Z.X. Zhu, W.X. Chen, *Carbon* 100 (2016) 408.
- [16] M. Silva, M.J. Calvete, N.P. Goncalves, H.D. Burrows, M. Sarakha, A. Fernandes, M.F. Ribeiro, M.E. Azenha, M.M. Pereira, J. Hazard. Mater. 233–234 (2012) 79.
- [17] Z. Han, X. Han, X. Zhao, J. Yu, H. Xu, *J. Hazard. Mater.* 320 (2016) 27.
- [18] M.T. Reetz, N. Jiao, *Angew. Chem. Int. Ed.* 45 (2006) 2416.
- [19] R. Tamura, T. Kawata, Y. Hattori, N. Kobayashi, M. Kimura, *Macromolecules* 50 (2017) 7978.
- [20] N.B. McKeown, P.M. Budd, *Chem. Soc. Rev.* 35 (2006) 675.
- [21] Z. Wang, G. Chem, K.L. Ding, *Chem. Rev.* 109 (2009) 322.
- [22] A.I. Cooper, *Adv. Mater.* 21 (2009) 1291.
- [23] P. Kaur, J.T. Hupp, S.T. Nguyen, *ACS Catal.* 1 (2011) 819.
- [24] D. Wu, F. Xu, B. Sun, R. Fu, H. He, K. Matyjaszewski, *Chem. Rev.* 112 (2012) 3959.
- [25] Y. Zhang, S.N. Riduan, *Chem. Soc. Rev.* 41 (2012) 2083.
- [26] X. Feng, X. Ding, D. Jiang, *Chem. Soc. Rev.* 41 (2012) 6010.
- [27] S.Y. Ding, W. Wang, *Chem. Soc. Rev.* 42 (2013) 548.
- [28] X. Zou, H. Ren, G. Zhu, *Chem. Commun.* 49 (2013) 3925.
- [29] J.L. Segura, M.J. Manchinoa, F. Zamora, *Chem. Soc. Rev.* 45 (2016) 5635.
- [30] E.L. Spitzer, W.R. Dichtel, *Nat. Chem.* 2 (2010) 672.
- [31] X.S. Ding, J. Guo, X. Feng, Y. Honsho, J.D. Guo, S. Seki, P. Maitarad, A. Saeki, S. Nagase, D. Jiang, *Angew. Chem. Int. Ed.* 50 (2011) 1289.
- [32] J.W. Colson, A.R. Woll, A. Mukherjee, M.P. Levendorf, E.L. Spitzer, V.B. Shields, M.G. Spencer, J. Park, W.R. Dichtel, *Science* 332 (2011) 228.
- [33] E.L. Spitzer, J.W. Colson, F.J. Uribe-Romo, A.R. Woll, M.R. Giovino, A. Saldivar, W.R. Dichtel, *Angew. Chem. Int. Ed.* 51 (2012) 2623.
- [34] A.V. Maffei, P.M. Budd, N.B. McKeown, *Langmuir* 22 (2006) 4225.
- [35] H.J. Mackintosh, P.M. Budd, N.B. McKeown, *J. Mater. Chem.* 18 (2008) 573.
- [36] M.P. Castaldi, S.E. Gibson, M. Rudd, A.J.P. White, *Chem. Eur. J.* 12 (2006) 138.
- [37] B.N. Achar, K.S. Lokesha, J. Organomet. Chem. 689 (2004) 3357.
- [38] F.J. Uribe-Romo, J.R. Hunt, H. Furukawa, C. Klock, M. O'Keeffe, O.M. Yaghi, *J. Am. Chem. Soc.* 131 (2009) 4570.
- [39] F.J. Uribe-Romo, C.J. Doonan, H. Furukawa, K. Oisaki, O.M. Yaghi, *J. Am. Chem. Soc.* 133 (2011) 11478.
- [40] J.S. Jung, J.W. Lee, K. Kim, M.Y. Cho, S.G. Jo, J. Joo, *Chem. Mater.* 22 (2010) 2219.
- [41] J. Tauc, *Mat. Res. Bull.* 3 (1968) 37.
- [42] O.V. Zalomaeva, K.A. Kovalenko, Yu.A. Chesarov, M.S. Mel'gunov, V.I. Zaikovskii, V.V. Kaichev, A.B. Sorokin, O.A. Kholdeeva, V.P. Fedin, *Dalton Trans.* 40 (2011) 1441.
- [43] R. Cao, R. Thapa, H. Kim, X. Xu, M. Gyu Kim, Q. Li, N. Park, M. Liu, J. Cho, *Nat. Commun.* 4 (2013) 2076.
- [44] J.A. Labinger, J.E. Bercaw, *Nature* 417 (2002) 507.
- [45] W.D. Jones, *Science* 287 (2000) 1942.
- [46] J.E. Bäckvall, *Modern Oxidation Methods*, John Wiley, Weinheim, 2011.
- [47] T. Punniyamurthy, S. Velusamy, J. Iqbal, *Chem. Rev.* 105 (2005) 2329.
- [48] P. Dongare, I. MacKenzie, D. Wang, D.A. Nicewicz, T.J. Meyer, *PNAS* 114 (2017) 9279.
- [49] W. Zhang, A. Bariotaki, I. Smonou, F. Hollmann, *Green Chem.* 19 (2017) 2096.
- [50] D. Hamdane, H. Zhang, P. Hollenberg, *Photosynth. Res.* 98 (2008) 657.
- [51] Y. Ishii, S. Sakaguchi, T. Iwahama, *Adv. Synth. Catal.* 343 (2001) 393.
- [52] F.C. Recupero, F. Punta, *Chem. Rev.* 107 (2007) 3800.